Heteromerization of Innexin Gap Junction Proteins Regulates Epithelial Tissue Organization in *Drosophila*

Corinna Lehmann,* Hildegard Lechner,* Birgit Löer,* Martin Knieps,†
Sonja Herrmann,† Michael Famulok,† Reinhard Bauer,* and Michael Hoch*

*Institut für Molekulare Physiologie und Entwicklungsbiologie der Universität Bonn, 53115 Bonn, Germany;
and †Kekulé-Institut für Organische Chemie und Biochemie der Universität Bonn, 53121 Bonn, Germany

Gap junctions consist of clusters of intercellular channels, which enable direct cell-to-cell communication and adhesion in animals. Whereas deuterostomes, including all vertebrates, use members of the connexin and pannexin multiprotein families to assemble gap junction channels, protostomes such as *Drosophila* and *Caenorhabditis elegans* use members of the innexin protein family. The molecular composition of innexin-containing gap junctions and the functional significance of innexin oligomerization for development are largely unknown. Here, we report that heteromerization of *Drosophila* innexins 2 and 3 is crucial for epithelial organization and polarity of the embryonic epidermis. Both innexins colocalize in epithelial cell membranes. Innexin3 is mislocalized to the cytoplasm in *innexin2* mutants and is recruited into ectopic expression domains defined by innexin2 misexpression. Conversely, RNA interference (RNAi) knockdown of *innexin3* causes mislocalization of innexin2 and of DE-cadherin, causing cell polarity defects in the epidermis. Biochemical interaction studies, surface plasmon resonance analysis, transgenesis, and biochemical fractionation experiments demonstrate that both innexins interact via their C-terminal cytoplasmic domains during the assembly of heteromeric channels. Our data provide the first molecular and functional demonstration that innexin heteromerization occurs in vivo and reveal insight into a molecular mechanism by which innexins may oligomerize into heteromeric gap junction channels.

INTRODUCTION

Gap junctions contain arrays of intercellular channels, which regulate direct cell-to-cell communication during development and homeostasis (Goodenough *et al.*, 1996; Wei *et al.*, 2004). They form spatial microdomains in the plasma membrane at regions of cell adhesion and enable the integration of metabolic and signaling activities by allowing the direct exchange of ions and small molecules among neighboring cells. For the formation of a functional gap junction channel, two hexameric hemichannels, one contributed by each of the opposing cells, dock head to head in the extracellular space to form a double membrane-spanning intercellular channel (Segretain and Falk, 2004; Martin and Evans, 2004).

Three unrelated gene families have evolved to construct gap junction channels, the *connexins* and *pannexins* in deuterostomes, including all vertebrates, and the *innexins* in protostomes, including the invertebrates *Drosophila* and *Caenorhabditis elegans* (Phelan *et al.*, 1998a; Söhl and Willecke, 2004; White *et al.*, 2004; Bauer *et al.*, 2005; Phelan, 2005). All three gene families encode four-pass membrane domains with two extracellular loops, cytoplasmic N and C termini, and a cytoplasmic loop domain. The *connexin* multigene family consists of 20 members in mice and 21 members in humans, and its contribution to intercellular communication has been extensively studied (Goodenough *et al.*, 1996; Söhl

and Willecke, 2004; Wei *et al.*, 2004). Three pannexin genes with distinct expression patterns in the brain have been recently identified in mouse and humans (Panchin *et al.*, 2000; Bruzzone *et al.*, 2003; Baranova *et al.*, 2004; Panchin, 2005). Genome sequencing projects identified eight *innexin* genes in the fruit fly *Drosophila* and 25 in the nematode *C. elegans* (Phelan and Starich, 2001). Connexin and pannexin genes are lacking in the fly and the nematode. Meanwhile, *innexin* genes have been cloned from several other invertebrate species including the cnidarian *Hydra vulgaris* (Alexopoulos *et al.*, 2004), suggesting that *innexins* may encode gap junction proteins in all protostomes. Although innexins, connexins, and pannexins are structurally and functionally analogous, they show very little sequence similarity to each other.

For the eight *innexin* genes known in *Drosophila*, functions have been assigned via mutant and expression analysis to *ogre* and *shakingB* in the adult visual system (Watanabe and Kankel, 1992; Krishnan *et al.*, 1993; Phelan *et al.*, 1996, 1998b; Shimohigashi and Meinertzhagen, 1998; Zhang *et al.*, 1999; Jacobs *et al.*, 2000; Curtin *et al.*, 2002) and to *innexin4* (*zero population growth*) in germ cell differentiation (Tazuke *et al.*, 2002; Gilboa *et al.*, 2003). *innexin2* (*kropf*) is required for the organization of epithelial cell layers in various organs, including the developing epidermis and the foregut (Bauer *et al.*, 2002, 2004). No functional data are available to date on innexins 3, 5, 6, and 7. Mutations in *connexin* genes have been linked to a variety of human disorders, including peripheral neuropathy, nonsyndromal deafness, and cardiovascular anomalies (reviewed in Wei *et al.*, 2004).

Both connexins and innexins are expressed in complex and overlapping expression patterns during development,

and most cells and tissues express more than one connexin or innexin isoform. This enables cells to assemble homomeric (composed of identical subunits) or heteromeric (composed of different subunits) hemichannels resulting in the formation of homotypic (two hemichannels are identical) or heterotypic (two hemichannels differ in molecular composition) intercellular channels that may provide greater complexity in the regulation of gap junction communication (Cottrell and Burt, 2005). Although many examples for heteromeric/heterotypic connexin channels have been demonstrated in the heterologous *Xenopus* oocyte system, in tissue culture cells and also in a few cases in vivo, to what degree connexin hetero-oligomerization occurs in vivo and what physiological function it serves has still remained unclear. Similarly, expression of Shaking B-lethal and innexin2 in the heterologous *Xenopus* oocyte expression system and subsequent electrophysiological studies have demonstrated the potential for these two innexins to form homotypic channels, whereas innexin3 and innexin2 were shown to have the capacity to form heteromeric channels (Stebbings *et al.*, 2000). However, it is not clear whether homomeric or heteromeric innexin channels occur in vivo, and if so, how they are assembled and what function they may serve during tissue and organ development.

MATERIALS AND METHODS

Genetic Manipulation of Flies

We used standard techniques for fly manipulation. For mutant analysis, we used kropf[P16] alleles (Bauer *et al.*, 2002). Ectopic innexin (inx) expression studies were performed at 29°C using UASinx2, UASinx2-GFP, UASinx3-GFP, and UASwizinx3 (see below) as effector lines and *paired*-Gal4 and *69B*-Gal4 as driver lines (Brand and Perrimon, 1993; Xiao *et al.*, 1996; Bauer *et al.*, 2004).

Antibody Generation

The peptide CPDDYRRDRQDRILKY containing the aa 157–171 of the inx3 protein sequence was synthesized, coupled to keyhole limpet hemocyanin (KLH), and used to generate an affinity-purified anti-inx3 rabbit polyclonal antibody. Synthesis and immunization was done in rabbits by Davids Biotechnology (Regensburg, Germany), using standard protocols.

Antibody Stainings and In Situ Hybridization

For in situ hybridization, the entire *inx3* mRNA was subcloned into the EcoRI/XhoI sites of the pScript vector. Full-length digoxygenin RNA antisense probes were generated by in vitro transcription and labeled during run off transcription according to the manufacturer's instructions (Roche Diagnostics, Mannheim, Germany). In situ hybridization and antibody stainings were performed using standard protocols as described by Bauer *et al.* (2001). As primary antibodies, we used anti-arm (1:20; Developmental Studies Hybridoma Bank, University of Iowa, Iowa City, IA), anti-inx2 rabbit (1:75; Bauer *et al.*, 2004), anti-inx2 chicken (1:50; anti-22C10 (1:10; Hybridoma Bank), anti-green fluorescent protein (GFP) (1:100; Roche Diagnostics), and anti-DE-cadherin (1:50; Santa Cruz Biotechnology, Santa Cruz, CA) and anti-inx3 (1:75). As secondary antibodies, we used Alexa 488 (1:100; MoBiTec, Göttingen, Germany); Alexa Fluor 546 (1:200; MoBiTec); Cy3, Cy2, and Cy5 (each 1:100; Dianova, Hamburg, Germany). Embryos stained with fluorescent antibodies were analyzed by laser scanning microscopy (Leica TSC2). Each fluorochrome was scanned individually to avoid cross-talk between channels. Images were subsequently combined using Adobe Photoshop 6.0 (Adobe Systems, Mountain View, CA).

Yeast Two-Hybrid Analysis and Plasmid Construction

The inx2 C terminus (CT) corresponding to the region from aa 289 (primer 5'-GGG ATC CCG AGA ATC GCT GTT GTG GCG GGT-3') to aa 367 (primer 5'-CGA GCT CGT TAG GCG TCG AAG GGC CGC-3') was amplified by PCR from LD11658 containing the entire inx2 cDNA. Subsequently, the amplification product was cut with BamHI and SacI and ligated in frame with the hSOS domain of the pSOS CytoTrap system vector (Stratagene, La Jolla, CA). It was used as bait, screening an embryonic library cloned in pMyr vectors and derived from the CytoTrap system (Stratagene). Screening was performed as described in the manual. Autoactivation of the inx3 target could be excluded after cotransformation of target and pSOS vector.

RNA Interference (RNAi) Experiments and pWIZ Constructs

A 620-base pair fragment (nucleotide 921-1540; GenBank accession no. AF172258) of inx3 was amplified and flanked with T7 binding motives by PCR (primer sequences: start, 5'-CTT TTA ATA CGA CTC ACT ATA GGG AGA GCT TGG CCA CCA TCT CCG GCG T-3'; stop, 5'-CTT TTA ATA CGA CTC ACT ATA GGG CTG GTA AAT GGT CCG TTA TTT AGG-3'). The fragment was used as template in the RiboMax Express Large Scale RNA Production system to produce complementary RNA of both strands. Injections were performed as described by Carthew (2001) with a final concentration of 0.5 μg/μl double-stranded RNA (dsRNA). Injections were performed with RNase-free needles into the posterior domain of the embryo at the syncytial blastoderm stage (injector Eppendorf TransferMan NK2). The volume ranged from 60 to 100 pl. Injection of buffer served as controls. For cuticle analyses embryos were incubated at 18°C under halocarbon oil for 48 h. The vitelline membrane was dissected, embryos were washed, and cuticles were prepared as described in Bauer *et al.* (2004). For in situ staining, devitellinized embryos were washed, fixed, and stained as described above.

To establish the stable transgenic UASwizinx3 knockdown lines, recombinant plasmids for the creation of stable RNAi-inducible fly strains were cloned as described by Lee and Carthew (2003). A 518-base pair DNA fragment of *inx3* (bases 668–1186 of the cDNA) was amplified by PCR and cloned into the AvrII and NheI of pWIZ vector (gift from R. W. Carthew, Northwestern University, Evanston, IL). Recombinants with inverted repeats of both orientations were selected. Recombinant plasmids were injected into white⁻ embryos, and transformant flies were generated by standard P element transformation (Spradling and Rubin, 1982) and crossed to Gal4 driver lines.

Cloning of Expression Vectors

Inx2 and 3 correspond to the following aa fragments: Inx2NT, aa 1–25; Inx2CL, aa 132–180; Inx2CT, aa 287–367; Inx3NT, aa 1–31; Inx3CL, aa 136–186; and Inx3CT, aa 293–395. The following primers were used to amplify inx domains toward cloning them into different expressions vectors (see below): BamInx2NTStart, 5'-CCG AGG ATC CAT ATG TTT GAT GTC TTT GGG TCC-3'; EcoInx2NTStop, 5'-GCG AAT TCC TAA TTG TTG TCG ATG CAC ACC TG-3'; BamInx2CLStart, 5'-CCG AGG ATC CAT AAG TCC TGG GAA GGC GGA-3'; EcoInx2CLStop, 5'-GCG AAT TCC TAT CGG AAG GCG TAG AAA TTG TG-3'; BamInx2CTStart, 5'-GGG ATC CCG AGA ATC GCT GTT GTG GCG GGT-3'; SacInx2CTStop, 5'-CGA GCT CGT TAG GCG TCG AAG GGC CGC-3'; EcoInx3NTStart, 5'-GGA ATT CCA TGG CGG TCT TTG GCA TGG TC-3'; XhoInx3NTStop, 5'-CCG CTC GAG CGG CGT GAT CCT GTA GTG GCA-3'; EcoInx3CSStart, 5'-GGA ATT CCA AGA ACA TGG AAG ACG GC-3'; XhoInx3CSStop, 5'-CCG CTC GAG CGG CGA GTA GCC GTT GTG G-3'; EcoInx3CTStart, 5'-GGA ATT CCT ATT CAC TGG TGG TTA TCA TG-3'; XhoInx3CTStop, 5'-CCG CTC GAG CGG TCA TGT CTC CGT CTC CTT-3'; and ApaInx3Stop, 5'-CGG GCC CGT GTC TCG GTC TCC TTG CCA CC-5'. The following primer was used to perform the insertion of a FLAG tag via PCR: 5'-CCG CCA CCG TTC CTC TGC CTC TGT CTA ATG TTC CTA CTG CTG CTA TTC TAG ACT GAG CTC GCC-3'. The following vectors were used to express tagged inx proteins: pMJGreen (kind gift from K. Willecke, University of Bonn, Bonn, Germany) for GFP-tagged inx2 and inx3; pGex5x-3 (GE Healthcare, Little Chalfont, Buckinghamshire, United Kingdom) for GST-tagged protein fragments; pQE-30Xa (QIAGEN, Valencia, CA) for His-tagged protein fragments; and pFast Bac (Invitrogen, Carlsbad, CA) for FLAG-tagged proteins. Proteins were expressed in *Escherichia coli* BL21 (Stratagene) cells or in case of InxCT FLAG-tagged protein in Sf21 cells.

Surface Plasmon Resonance Measurements

All SPR measurements were carried out with a BIAcore 3000 system (BIAcore, Uppsala, Sweden). Ligand proteins were coupled to final responses of 1.100 resonance units (RU) to 3.000 RU on CM5 sensor chips using the automated amino coupling procedure. For binding experiments and K_D measurements, the chip was equilibrated to $1 \times$ phosphate-buffered saline, pH 7.4, at 25°C. Injection of 120 μl of the analyte proteins glutathione *S*-transferase (GST), HisInx2CT, or GSTInx3CT was done at a constant flow rate of 30 μl/min. After 360 s of dissociation, the analyte was removed by injection of a short pulse 0.1% SDS in 5 mM NaOH as regeneration buffer. All binding curves were collected as double measurements and automatically subtracted from an underivatized reference surface. Obtained sensorgrams were analyzed with the BIAevaluation 3.1 software using the "steady-state affinity" fitting model.

Immunoprecipitation and Immunoblotting

Coimmunoprecipitation analyses of whole embryo lysates were performed using embryonic extracts of 0- to 16-h-old embryos and adult flies. The preparation of the extracts and the immunoprecipitation procedure was carried out as described in Bauer *et al.* (2004). Anti-inx3 and anti-inx2 antibodies were used at dilutions of 1:400 and anti-GFP antibody (Roche Diagnostics) at 1:1000. Secondary antibodies (anti-mouse and anti-rabbit; Dianova) were both used at a dilution of 1:2000 in 1% blocking solution (Roche Diagnostics).
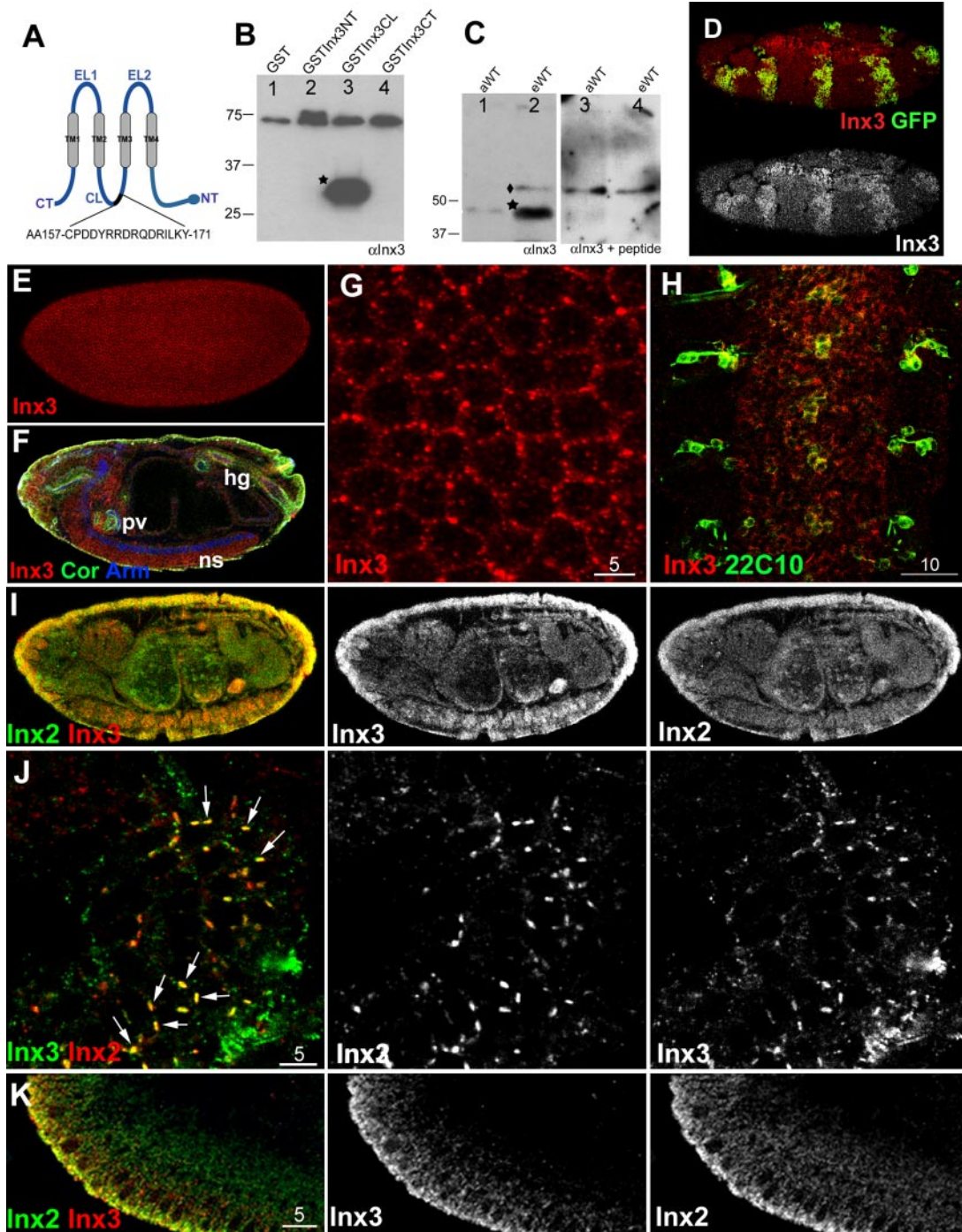
Figure 1. Coexpression of innexin3 and innexin2. (A) Predicted structure of inx3 protein with four transmembrane domains (TM), two extracellular loops (EL), an intracellular cytoplasmic loop (CL), and the intracellular N- and C-terminal domains (NT and CT). Amino acid sequence and localization of the inx3 peptide used for antibody production are indicated. (B) GST protein (control, lane 1) GSTInx3NT (lane 2), GSTInx3CL (lane 3), and GSTInx3CT (lane 4), detected with anti-inx3 antibody. Note that only in case of GSTinx3CL, a specific band of ~32 kDa (asterisk), corresponding to the size of the fusion protein of GST and the inx3CL, was detected, consistent with the origin of the epitope peptide used for immunization (NT, N terminus; CL, cytoplasmic loop; CT, C terminus). (C) Peptide competition experiments. Western blot using anti-inx3 antibody. Lanes 1 and 3, adult fly protein extract; lanes 2 and 4, embryonic extract of 0- to 16-h-old wild-type (wt) embryos. In lanes 1 and 2, a specific band of 45 kDa (asterisk) can be detected, corresponding to the predicted molecular mass of inx3. In lanes 3 and 4, the specific inx3 band is abolished upon competition with the epitope peptide (see *Materials and Methods*), whereas an unspecific band (rhomb) is still detectable. (D) Ectopic expression of inx3-GFP in seven stripes via the *paired*-GAL4 driver and the UASinx3-GFP effector lines. Note that the antibody detects ectopic innexin3 expression in the *paired* pattern of seven stripes (bottom), further demonstrating the specificity of the antibody. (E) Ubiquitous inx3 expression in a stage 5 embryo. (F) Triple staining monitoring expression of inx3 (red), coracle (green), and armadillo (blue) in a stage 16 wt embryo. Prominent inx3 staining is visible in the proventriculus, the hindgut, the epidermis (G), and the nervous system, as shown by costaining with the 22C10 marker, staining neuronal cells within the peripheral nervous system and CNS (H)(pv, proventriculus; ns, nervous system; hg, hindgut). (I) Costaining of inx2 and inx3 in wt embryos.

Innexin Coimmunoprecipitations from Triton X-100 (TX100)–soluble Fractions

Dechorionated 0- to 16-h-old wild-type embryos were homogenized with 20 strokes of a type B pestle on ice. Debris and nuclei were pelleted at $500 \times g$ for 10 min. The supernatant was incubated for 40 min with 1% TX100 on ice to separate TX100-insoluble gap junction plaques from newly synthesized innexin monomers and oligomers (Musil and Goodenough, 1993; Kistler *et al.*, 1994). The TX100-solubilized extract was separated from TX100-insoluble material by high-speed centrifugation at $100,000 \times g$. Proteins from these fractions were concentrated in Amicon Ultra-15 centrifugal filter devices (Millipore, Billerica, MA). The sample was diluted with radioimmunoprecipitation assay buffer to a final concentration of 1 µg of protein/µl. After additional homogenization with a 26-gauge syringe and treatment for 1 min in an ultrasonic bath followed by centrifugation for 15 min at $11,000 \times g$. The supernatant was divided in equal aliquots. Coimmunoprecipitation analysis was performed as described above and in Bauer *et al.* (2004).

RESULTS

Coexpression of Innexins2 and 3 in Developing Epithelia

It has been determined previously that the mRNA expression patterns of *innexin2* and *innexin3* are largely overlapping during embryogenesis (Stebbings *et al.*, 2000, 2002; Bauer *et al.*, 2001, 2002). Both innexins are expressed rather ubiquitously during the blastoderm stage and in a segmentally reiterated pattern in the epidermis during later stages of development. Most prominent coexpression is found in the developing fore- and hindgut and in the epidermis (Bauer *et al.*, 2002; Stebbings *et al.*, 2002). Innexin2 protein was found to be localized to the membrane of epithelial cells in an apico-lateral position, and mutant analysis has shown that innexin2 is required for the organization of epithelial cell layers (Bauer *et al.*, 2002, 2004). In contrast, functional studies on innexin3 are lacking because no *innexin3* mutants have been isolated. As a first step to study the developmental role of innexin3, we generated an anti-innexin3 antibody. We used the peptide CPDDYRRDRQDRILKY, which contains the amino acids 157–171 of innexin3 within the cytoplasmic loop for immunization (Figure 1A). The antibody detects a 45-kDa protein corresponding to the predicted size of innexin3 (Figure 1C); its specificity was determined by testing various GST fusion proteins representing different innexin3 protein domains (Figure 1B), and by peptide competition experiments using protein extracts of wild-type embryos and adult flies (Figure 1C). On overexpression of an innexin3-GFP construct in every other segment of the epidermis using *paired*-Gal4 driver and UASinx3-GFP effector transgenic flies (see *Materials and Methods*), the antibody detects the stripe pattern (Figure 1D), further demonstrating the specificity of the antibody.

Anti-innexin3 antibody staining of wild-type embryos shows that innexin3 protein is distributed in a punctuate pattern mainly at the plasma membrane and to some extent also within the cytoplasm of the epithelial cells from early embryonic stages onward (Figure 1, E–H). A similar kind of protein distribution was found for other innexins (Bauer *et al.*, 2001, Gilboa *et al.*, 2003) and for vertebrate connexins, which are localized in gap junctions in the membranes of the cells and within intracellular stores in the endoplasmic reticulum–Golgi interfacial regions (Laird, 1996). At later

Figure 1 (cont). Colocalization is most prominent in the hindgut (magnified in J) and the epidermis (magnified in K). Arrows in J depict sites of colocalization. We also find individual signals for both proteins that do not overlap (red and green signals), suggesting the occurrence of homomeric channels. Bars are in micrometers; anterior part of the embryo is shown to the left, ventral to the bottom.

stages of embryonic development, innexin3 is most prominently expressed in the epidermis, the developing fore- and hindgut, and in the central nervous system (CNS), as determined by using antibody double stainings with tissue-specific markers (Figure 1, F–H).

From blastoderm stage onwards until late stages of embryonic development, we find coexpression of innexins 2 and 3 in most tissues (Figure 1, I–K). Both proteins are colocalized in the membrane of epithelial cells, e.g., in the developing hindgut (Figure 1J) and in epidermal cells, from very early stages onward (Figure 1K). It is noteworthy, however, that we also find nonoverlapping signals of both innexins, which may indicate homomeric channels (Figure 1J).

Innexin3 Knockdown Causes Innexin2-like Mutant Phenotypes

We have previously shown that in maternal and zygotic null mutants of *innexin2* (*kropf* mutants), epithelial morphogenesis is severely disrupted, resulting in cuticle holes and loss of cuticle formation in the most extreme cases (Bauer *et al.*, 2002, 2004). During epidermal development, innexin2 was found to colocalize with armadillo and DE-cadherin, which are core proteins of adherens junctions (reviewed in Wheelock and Johnson, 2003) and evidence for direct molecular interactions between innexin2, DE-cadherin, and armadillo could be obtained in vitro and in vivo (Bauer *et al.*, 2004). These data suggested that the positioning of gap junctions may depend on adherens junction proteins.

To further test the function of innexin3, we performed RNAi experiments to knock down *innexin3* mRNA expression (Figure 2). We first injected 620-base pair dsRNA fragment into the posterior part of stage 3 embryos. In these embryos, *innexin3* transcripts were strongly reduced, and we observed severe cuticle defects in the injected embryos, reflecting misdevelopment of the epidermis (our unpublished data). To investigate this in more detail, we generated a transgenic line carrying an UAS/Gal4 RNAi construct for innexin3 (UASwizinx3) in which part of its coding regions was cloned into a "face-to-face" orientation (Figure 2A). Using the UASwizinx3 effector in combination with the driver lines *paired*-Gal4, which knocks down *innexin3* mRNA expression in every other segment (Figure 2D, compare with wild type in 2B), or *69B*-Gal4, which mediates knockdown ubiquitously in the epidermis (Figure 2F), we find cuticle phenotypes similar to the dsRNA injection experiments: holes and irregular denticle belts or a complete loss of cuticle in the most extreme cases (Figure 2, E and G, compare with wild type in C). It is of note that *kropf* mutant embryos show similar defects during epidermis development (Bauer *et al.*, 2004). In earlier developmental stages, the membrane localization of innexin2 is severely affected in *69B*-Gal4 × UASwizinx3 knockdown embryos, and innexin2 protein accumulates to a considerable extent in the cytoplasm (Figure 2H, compare with wild type in inset of H). The distribution of the adherens junction core proteins DE-cadherin and armadillo (our unpublished data) is also changed in these embryos, from an apico-lateral localization in wild type to an accumulation in a more lateral membrane domain in the mutants (Figure 2, J and L, compare with wild type in I, K, and M); consistently, we observe a rounding up of the affected cells, characteristic for cell polarity defects (Tepass *et al.*, 1996; Uemura *et al.*, 1996). These data suggest an essential role for innexin3 in proper epithelial development of the epidermis, and they indicate that it controls innexin2 membrane localization, explaining the close similarity of the mutant defects of *innexin3* knockdown and *innexin2* mutant embryos. Conversely, we find innexin3 membrane localiza-

Figure 2. Functional analyses of innexin3 and innexin2 in vivo. (A) Scheme of the inducible inx3 knockdown construct UASwizinx3. (B) In situ hybridization experiments showing inx3 mRNA expression in wt embryos. (C) Cuticle preparation of wt embryos. (D) RNAi-dependent knockdown of inx3 using the *paired*-Gal4 driver and UASwizinx3 effector; *inx3* expression is downregulated in every other segment (arrows). The asterisk depicts the expression domain of an internal staining control *orthopedia* (*otp*; Bauer *et al.*, 2002). (E) Cuticle preparation of *paired*-Gal4 × UASwizinx3 embryos; arrowhead indicates a large hole in the cuticle, and arrows indicate irregular denticle belts reflecting misdevelopment of the epidermis. (F) RNAi-dependent downregulation of inx3 using the ubiquitously expressing epidermal driver *69B*-Gal4 and the UASwizinx3 effector. A cuticle preparation of these embryos (G) shows a barely developed cuticle. (H) Top view and (J) lateral view of an anti-inx2 (red)/anti-DE-cadherin (green) double staining in the epidermis of *69B*-Gal4 × UASwizinx3 embryos of stage 6. Most cells lost their polarity and inx2 is accumulated within the cytoplasm (arrows in H).

tion affected in *innexin2* mutants (Figure 2N, compare with wild type in I) and when innexin2 is misexpressed in stripes using an UASinx2 effector and a *paired*-Gal4 driver line, innexin3 is recruited into the ectopic expression domains of innexin2 (Figure 2O). In summary, the coexpression data, the similarities of the innexin2 and innexin3 mutant phenotypes and the observation that membrane localization of innexin2 is altered in *innexin3* mutants and vice versa, strongly suggest the possibility that innexin2 and innexin3 may interact with each other to form heteromeric channels. To obtain further evidence for hetero-oligomerization of both innexins and to identify interacting protein domains, we carried out a series of molecular and biochemical experiments.

Direct Interaction of Innexin2 with Innexin3

In a yeast two-hybrid interaction screen using the C-terminal cytoplasmic domain of innexin2 as a bait, we identified innexin3 as an interaction partner, providing the first molecular evidence that both innexins directly interact (Figure 3A). We screened a 0- to 24-h-old embryonic library derived from the CytoTrap system. After screening $\sim 10^8$ transformants and incubation at 37°C for 5 d, 34 potential positive clones were isolated of which 10 clones could be confirmed in a rescreen (Lehmann and Hoch, unpublished data). Among them was one clone containing the entire *innexin3* cDNA. To confirm the yeast two-hybrid data, we performed coimmunoprecipitation analysis by using anti-innexin2 and anti-innexin3 antibodies in combination with embryonic extracts of wild-type embryos. As shown in Figure 3C, innexin3 can be precipitated specifically by using anti-innexin2 antibodies and vice versa (Figure 3D). When using extracts of transgenic embryos, which express a C-terminal-tagged innexin2-GFP fusion protein or when deleting the C-terminal domain, the interaction with innexin3 fails to occur (Figure 3E; our unpublished data). Consistent with the coimmunoprecipitation data, we find that in transgenic embryos expressing the innexin2-GFP fusion protein, innexin3 is not colocalized to innexin2-GFP (Figure 3G, compare with wild type in F). Consistently, overexpression of innexin2-GFP does not recruit innexin3 into the ectopic expression domains (Figure 3, I and J), and cells do not loose their polarity and do not round up (Figure 3H). These data further underline the significance of the C-terminal cytoplasmic domain of innexin2 for the interaction with innexin3.

The C Terminus of Innexin3 Interacts with Innexin2 and With Its Own Cytoplasmic Loop

To identify the domains with which innexin3 interacts with the C terminus of innexin2 and to quantify the interactions, we carried out surface plasmon resonance measurements. We tagged three cytoplasmic domains of innexin3: the N

The inset in H shows a wt staining of inx2 localized in the membranes of epidermal cells, for comparison. Note also the mislocalization of DE-cadherin (arrow in J) in the *69B*-Gal4 × UASwizinx3 embryos; this is better visible when the DE-cadherin channel is shown only (L) compared with wt DE-cadherin staining in M. Top view (I) and lateral view (K) of an inx3 (red)/DE-cadherin (green) double staining in the epidermis of wt embryos of stage 6. (M) DE-cadherin staining of epidermal cells in wt embryos. (N) Double staining of epidermal cells in *kropf* mutants monitoring inx3 (red) and armadillo (green). The polarity of the cells is affected and inx3 is mislocalized within the cell (compare with wt in I). (O) Inx2/inx3 double staining of *paired*-Gal4 × UASinx2 embryos. Note that inx3 is recruited to the inx2 overexpressing cells. Bars are in micrometers.

Figure 3. Direct interaction of innexin2 and innexin3. (A) Scheme of bait and target protein of the yeast two-hybrid screen. Inx2CT (aa 288–368) was used as bait, and full-length inx3 was found as target protein, both depicted in red. (B) Confirming yeast experiments. I, negative control; II, positive control; III, cotransformation of target and pSOS vector; and IV, cotransformation of bait and target; three colonies each are shown. (C–E) Coimmunoprecipitation of inx2 and inx3 (bands depicted by a rhomb correspond to the size of antibody IgG bands). (C) Anti-inx3 was used as precipitating antibody and anti-inx2 as detecting antibody. Lane 1, embryonic wt extract, inx3 (45 kDa; star); lane 2, coimmunoprecipitation; and lane 3, negative control. (D) Anti-inx2 was used as precipitating antibody and anti-inx3 as detecting antibody. Lane 1, embryonic wt extract inx2 (43 kDa; star); lane 2, coimmunoprecipitation; and lane 3, negative control. (E) Anti-inx3 was used as precipitating antibody and anti-GFP as detecting antibody. Lane 1, embryonic $V32$Gal4 × UAS-inx2-GFP extract; inx2-GFP (68.5 kDa; star); lane 2, coimmunoprecipitation; and lane 3, negative control. Note the interaction of inx2 and inx3 is abolished using the C-terminal–tagged inx2-GFP protein. (F) Double staining monitoring expression of inx3 (red) and inx2 (green) in the epidermis of wild-type embryos. (G) Double staining of inx3 (red) and inx2GFP (green) in *arm*-Gal4 × UASinx2 embryo expression. Note colocalization of inx3 and inx2-GFP is not seen. (H) Double staining of *paired*-Gal4 x UASinx2-GFP embryos monitoring the fusion protein inx2GFP (green) and arm (red). Note epidermal cell shape is not affected in inx2-GFP–expressing cells. (I and J) Overview of a *paired*-Gal4 × UASinx2-GFP embryo, GFP in green (I) and inx3 in red (J). Note inx3 expression is not recruited into every other stripe, compared with Figure 2O. Bars are in micrometers.
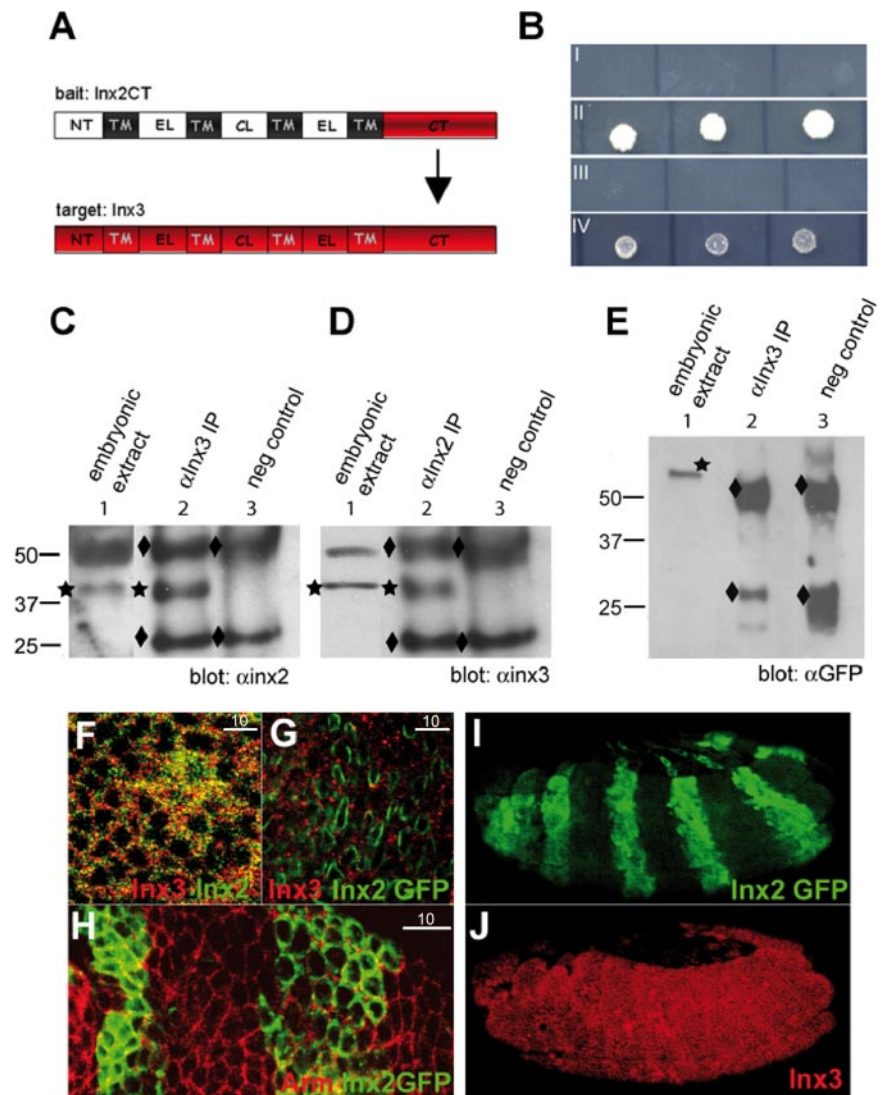
terminus, the cytoplasmic loop, and the C terminus (summarized in Figure 4A) and immobilized those fusion proteins on the sensor chip. We then incubated the chip with the His-tagged version of the C terminus of innexin3. We found that the C terminus of innexin2 showed concentration-dependent binding to the C-terminal domain of innexin3 in the low micromolar range (with a K_D of 2.45 μM; Figure 4B), consistent with our previous yeast two-hybrid and coimmunoprecipitation experiments. Interactions of the C terminus of innexin2 with other protein domains of innexin3 could not be observed. The binding of both C termini to each other could be confirmed in the reverse experiment, immobilizing the C terminus of innexin2 to the chip as the ligand and using the C terminus of innexin3 as analyte protein (summarized in Figure 4A). In contrast to the selective binding behavior of the innexin2 C terminus, the C terminus of innexin3 has the potential to interact more broadly. We find heteromeric interactions with the cytoplasmic loop domain of innexin2 (K_D of 1.74 μM; Figure 4C) and homomeric interactions with its N terminus (K_D of 3.13 μM; Figure 4D) and its cytoplasmic loop (K_D of 2.65 μM; Figure 4E). In

summary, the surface plasmon resonance data demonstrate and further confirm the potential of innexin2 and innexin3 to hetero-oligomerize in vitro via their cytoplasmic domains.

Innexin2 and Innexin3 Form Heterodimers In Vivo

To test whether innexin2 and innexin3 form heteromers in vivo, we performed biochemical fractionation experiments. We prepared embryonic extracts of 0- to 16-h-old wild-type embryos and used high-speed centrifugation in combination with coimmunoprecipitation to study intracellular innexin2/innexin3 heteromerization. We used a protocol that was previously applied to study the assembly of connexin proteins into oligomeric channels (Musil and Goodenough, 1993; Kistler *et al.*, 1994). In this procedure, insoluble gap junction plaques located at the plasma membrane are separated from newly synthesized innexin monomers and oligomers located in the cytoplasmic fraction, by Triton X-100 treatment and centrifugation (Figure 5A). In coimmunoprecipitation experiments using the Triton X-100–soluble fraction, which includes all intracellular intermediate assembly
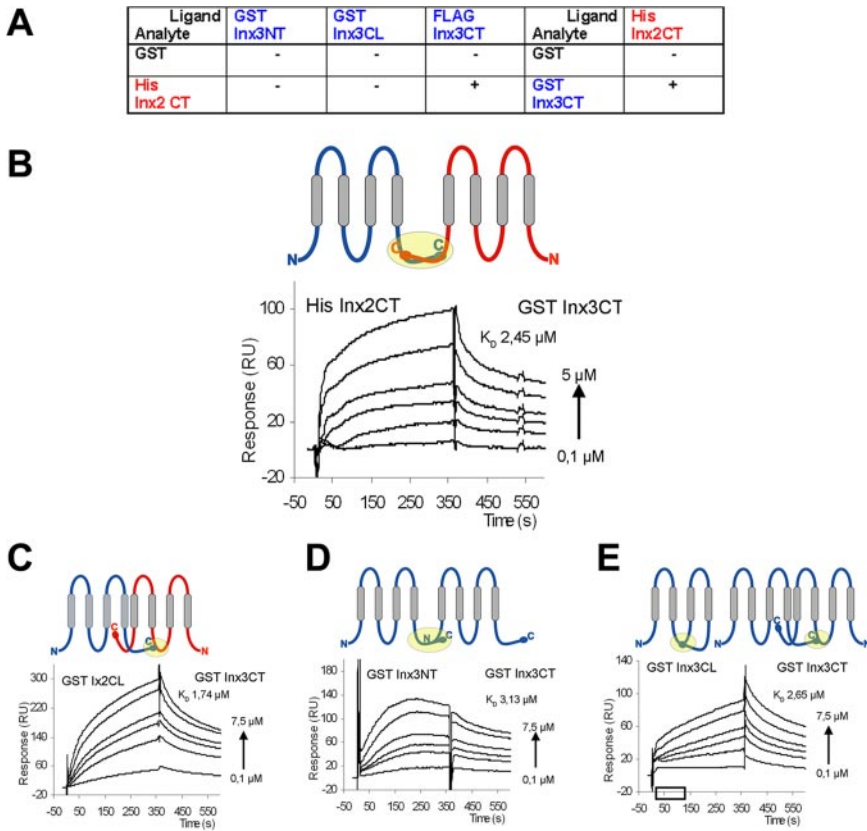
Figure 4. Surface plasmon resonance experiments of cytoplasmic innexin2 and innexin3 domains. (A) Table gives an overview of the protein domains of inx2 and inx3 tested and for positive (+) or negative (−) interactions. All interactions were independently confirmed by interchange of analyte and ligand proteins (our unpublished data). (B–E) Models (top) and sensorgrams (bottom) for discovered interactions (see text and *Materials and Methods*).

products of gap junction channels, innexin2 is specifically coimmunoprecipitated by anti-innexin3 antibody and vice versa (Figure 5B). These data strongly suggest that innexins 2 and 3 form heteromers in vivo during the assembly of heteromeric channels.

DISCUSSION

Gap Junctions contain clusters of intercellular channels, which allow the direct exchange of ions and small molecules among neighboring cells, thus enabling cells and tissues to integrate signaling activities. Whereas the biosynthesis, oligomerization, trafficking, and turnover of connexin channels and their multiple functions in development and homeostasis of vertebrates are well studied (reviewed in Wei *et al.*, 2004 and Segretain and Falk, 2004), the molecular composition of innexin-containing gap junctions and the functional significance of innexin oligomerization in developmental

processes is unknown (reviewed in Bauer *et al.*, 2005 and Phelan, 2005). We have used a combination of in vitro approaches, including yeast two-hybrid analysis, coimmunoprecipitation, and surface plasmon resonance studies, and in vivo analysis, including the study of mutants, RNAi knockdown embryos, and transgenic animals to investigate the role of the *Drosophila* innexins 2 and 3 during embryonic development. Our results provide strong evidence that both innexins are essential for epidermis development and that they form heteromers via C termini-mediated interactions, suggesting a mechanism of how innexins may oligomerize into heteromeric gap junction channels.

Innexins2 and 3 Are Essential for Epithelial Tissue Morphogenesis
Our coimmunostainings indicate that innexins 2 and 3 are colocalized in the membrane of epidermal cells, and our
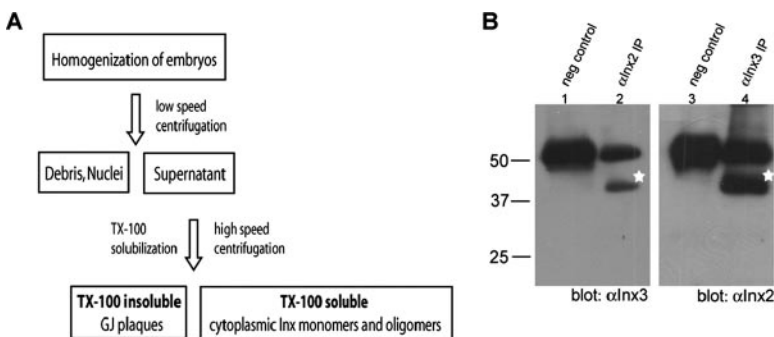
Figure 5. Innexin2 and innexin3 interact within the cytoplasm. (A) Flow chart describing the separation by Triton X-100 treatment and centrifugation of insoluble gap junction plaques located at the plasma membrane and newly synthesized innexin monomers and oligomers located in the cytoplasmic fraction (Musil and Goodenough, 1993; Kistler *et al.*, 1994). (B) Coimmunoprecipitaion analyses with a Triton X-100–soluble fraction. Left, anti-inx2 was precipitating antibody; right, anti-inx3 was precipitating antibody. Lanes 1 and 3, negative control; lanes 2 and 4, coimmunoprecipitation with protein extract from a Triton X-100–soluble fraction, containing newly synthesized innexin monomers and oligomers; stars depict either innexin3 (left) or innexin2 (right)-specific bands. All other bands correspond to the size of antibody IgG bands.

Figure 6. Model describing the heteromerization and the function of innexins 2 and 3 in epithelial cells of the *Drosophila* embryo. Left, both innexins colocalize in epithelial cell membranes of wild-type embryos; their heteromerization, which is mediated via interaction of their C-terminal cytoplasmic domains, is crucial for epithelial organization and the polarity of the epidermal cells. Middle, Innexin2 is mislocalized to the cytoplasm in *innexin3* knockdown embryos, and adherens junction proteins such as DE-cadherin or armadillo are mislocalized, resulting in cell polarity defects. Right, conversely, innexin3 and DE-cadherin are mislocalized in *innexin2* mutants, causing cell polarity defects in the epidermis similar to *innexin3* knockdown embryos.
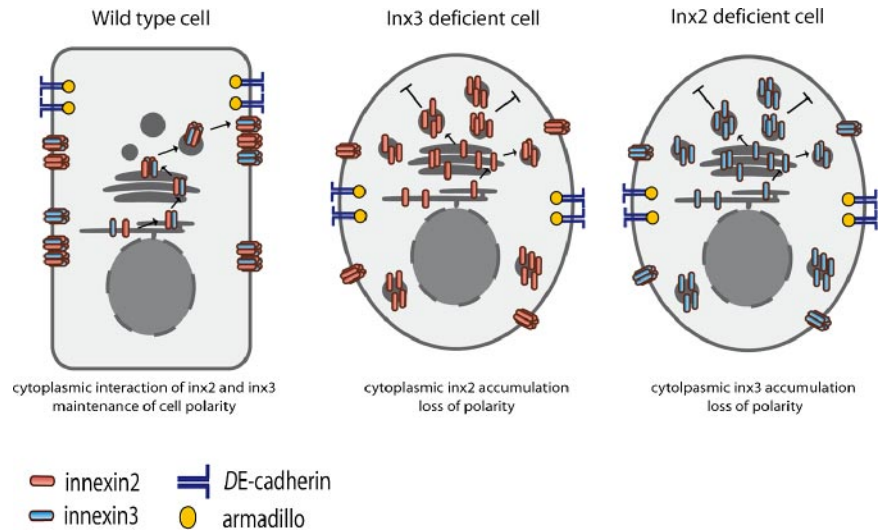
genetic loss and gain-of-function experiments show that membrane localization and cellular distribution of both innexins is mutually dependent on each other (Figure 6): innexin2 is mislocalized to the cytoplasm upon RNAi knockdown of *innexin3*, and innexin3 is mislocalized to the cytoplasm in *innexin2* mutants (Figure 2, H and N). Furthermore, innexin3 is recruited into ectopic expression domains defined by misexpression of innexin2. Consistent with the dependence of both innexins on each other, mutants or RNAi knockdown of either of the genes shows very similar cell polarity defects in the epidermis: on RNAi knockdown of *innexin3* or in *innexin2* mutants, we find large holes in the cuticle or even a complete loss of cuticle in the most extreme cases (Figure 2, E and G; Bauer *et al.*, 2004), the proper membrane distribution of DE-cadherin is affected in the mutant embryos, and we observe a rounding up of the affected cells, characteristic for cell polarity defects (Figure 2L; Tepass *et al.*, 1996; Uemura *et al.*, 1996). These data suggest that heteromerization of both innexins is essential for proper epithelial development of the epidermis. It has been shown previously that innexin2 protein accumulates in the apico-lateral membrane domain and colocalizes with armadillo and DE-cadherin (Bauer *et al.*, 2004). In mutants for both zygotic *armadillo* and DE-cadherin, the localization of innexin2 is altered and in innexin2 overexpression experiments, armadillo and DE-cadherin are organized into the ectopic innexin2 pattern. Further evidence for a more direct interaction between innexin2 and adherens junction proteins was provided by yeast two-hybrid analysis and coimmunoprecipitation experiments using embryonic extracts, which showed that innexin2 interacts via its cytoplasmic loop domain with the C terminus of DE-cadherin (Bauer *et al.*, 2004). It is not clear whether innexin3 also directly binds to DE-cadherin or whether the heteromeric interactions of innexin3 with innexin2 explain the alterations of DE-cadherin localization in *innexin3* knockdowns in which innexin2 is mislocalized. Also, we cannot exclude that the cell polarity defects observed in *innexin* knockdown embryos are an indirect consequence of defective cell-to-cell communication among epidermal cells. However, we currently favor the possibility that interactions between DE-cadherin and innexins may reflect common trafficking routes of adherens junction and gap junction proteins within cells that ensure the positioning of innexin-containing hemichannels in membrane domains close to adherens junctions in cells of the epidermis. This is

supported by recent data in the *Drosophila* Schneider cell system showing that DE-cadherin controls trafficking and localization of innexin2 to the plasma membrane (Bauer *et al.*, 2006). It was recently shown for the mammalian connexin43 α1 that it coassembles in a multiprotein complex containing N-cadherin and various N-cadherin–associated proteins, and it was suggested that the intracellular coassembly of connexins and cadherin is required for gap junction and adherens junction formation (Wei *et al.*, 2005). In mammals as in *Drosophila*, there thus seems to be an intimate linkage between the assembly of connexin-containing gap junctions and adherens junctions. This is supported by a number of studies in mammals, which have shown that the formation of connexin-containing gap junctions is dependent on the assembly of adherens junctions (Meyer *et al.*, 1992; Frenzel and Johnson, 1996; Hertig *et al.*, 1996; Luo and Radice, 2003). Inhibition of cadherin function can disrupt gap junction formation and inhibit cell–cell coupling, suggesting that localization of cadherin to cell–cell contact sites may be a prerequisite for gap junction formation (Meyer *et al.*, 1992). Conversely, inhibition of connexin43 can block adherens junction formation (Zuppinger *et al.*, 2000).

Innexins 2 and 3 Form Heteromers during Channel Assembly via C-Terminal Domain-mediated Interactions

Our yeast two-hybrid analysis, the coimmunoprecipitation and surface plasmon resonance studies, the biochemical fractionation experiments, and the in vivo analysis using transgenic embryos strongly suggest that the heteromeric interaction of both innexins occur during heteromeric channel assembly and are mediated via the cytoplasmic C-terminal domains of both innexins. Our data provide evidence that the heteromer of both proteins may be the smallest assembly unit during the formation of heteromeric innexin2/innexin3 channels. Coimmunoprecipitation analyses of full-length and progressively truncated versions of connexins 43, 32, and 26 have suggested the presence of isoform-specific intrinsic signals that regulate hetero-oligomerization of connexins (Falk *et al.*, 1997; Falk, 2000). An assembly signal allowing connexin subunits to recognize each other is supposed to be located in the third transmembrane domain, whereas a selectivity signal regulating subunit compatibility is located in the N-terminal domain and the first transmembrane domain (for reviews, see Lagree *et al.*, 2003 and Segretain and Falk, 2004). The corresponding

regions are not conserved on the amino acid sequence level between connexins and innexins, and it is not clear whether such signals also exist for innexins. Rather, our data suggest that heteromerization of innexins 2 and 3 is mediated by C-terminal interactions. In normal development, the heteromeric interactions of both innexins may be required for proper vesicular transport and membrane insertion of mixed hemichannels, because we observe an accumulation of innexin3 in the cytoplasm of epithelial cells of *kropf* mutants and vice versa. Specific heteromerization signals may exist in the C termini of both proteins determining isoform compatibility. It is known for connexins that hemichannel assembly is not a random process but rather can be regulated in a cell-specific manner (Das Sarma *et al.*, 2001). Furthermore, connexins do not contain conventional signal sequences for trafficking and assembly, thereby opening the option of multiple routes for trafficking and assembly in the same cell (Diez *et al.*, 1999). It is interesting to note from our BIAcore experiments that the C terminus of innexin2 seems much more restricted in its interaction range than the C terminus of innexin3, which interacts also with its own cytoplasmic loop and its own N terminus, suggesting the potential to form homomeric innexin3 channels. This may allow the regulation of heterotypic innexin 2/innexin 3 channels via a "ball and chain" mechanism that was proposed previously for the chemical gating of connexin43 (Delmar *et al.*, 2000) and requires the interaction of the carboxyl tail of connexin43 with its intracellular loop. Previous studies in the heterologous *Xenopus* expression system have shown that innexin2 can form homomeric channels in frog oocytes, whereas homomeric innexin3 channels were not functional (Stebbings *et al.*, 2000). In our coimmunostainings, we find some individual, nonoverlapping signals for both innexin2 and innexin3 in epithelial cells, suggesting that homomeric channels for innexin2 and 3 also exist in vivo (Figure 1J). The function of these channels is, however, not known. In summary, our results demonstrate that innexin heteromerization is crucial for epithelial tissue morphogenesis and polarity in *Drosophila* epidermis development. The binding of both innexins via their C termini provides a mechanism for oligomerization of heteromeric channels. In view of the evolutionary conservation of innexins in many protostomal species, including grasshoppers, molluscs, flatworms, polychaete annelids, leeches, protochordates, and cnidarians (for reviews, see Alexopoulos *et al.*, 2004 and Bauer *et al.*, 2005), our findings suggest that innexins may have an evolutionary conserved role in tissue morphogenesis and polarity in animals.

ACKNOWLEDGMENTS

REFERENCES

Alexopoulos, H., *et al.* (2004). Evolution of gap junctions: the missing link? Curr. Biol. *14*, R879–R880.

Baranova, A., *et al.* (2004). The mammalian pannexin family is homologous to the invertebrate innexin gap junction proteins. Genomics *83*, 706–716.

Bauer, R., Lehmann, C., Fuss, B., Eckardt, F., and Hoch, M. (2002). The *Drosophila* gap junction channel gene innexin 2 controls foregut development in response to Wingless signalling. J. Cell Sci. *115*, 1859–1867.

Bauer, R., Lehmann, C., and Hoch, M. (2001). Gastrointestinal development in the *Drosophila* embryo requires the activity of innexin gap junction channel proteins. Cell Commun. Adhes. *8*, 307–310.

Bauer, R., Lehmann, C., Martini, J., Eckardt, F., and Hoch, M. (2004). Gap junction channel protein innexin 2 is essential for epithelial morphogenesis in the *Drosophila* embryo. Mol. Biol. Cell *15*, 2992–3004.

Bauer, R., Loer, B., Ostrowski, K., Martini, J., Weimbs, A., Lechner, H., and Hoch, M. (2005). Intercellular communication: the *Drosophila* innexin multiprotein family of gap junction proteins. Chem. Biol. *12*, 515–526.

Bauer, R., Weimbs, A., and Hoch, M. (2006). DE-cadherin, a core component of the adherens junction complex modifies subcellular localization of the *Drosophila* gap junction protein innexin2. Cell Commun. Adhes. (*in press*).

Brand, A. H., and Perrimon, N. (1993). Targeted gene expression as a means of altering cell fates and generating dominant phenotypes. Development *118*, 401–415.

Bruzzone, R., Hormuzdi, S. G., Barbe, M. T., Herb, A., and Monyer, H. (2003). Pannexins, a family of gap junction proteins expressed in brain. Proc. Natl. Acad. Sci. USA *100*, 13644–13649.

Carthew, R. W. (2001). Gene silencing by double-stranded RNA. Curr. Opin. Cell Biol. *13*, 244–248.

Cottrell, G. T., and Burt, J. M. (2005). Functional consequences of heterogeneous gap junction channel formation and its influence in health and disease. Biochim. Biophys. Acta *1711*, 126–141.

Curtin, K. D., Zhang, Z., and Wyman, R. J. (2002). Gap junction proteins expressed during development are required for adult neural function in the *Drosophila* optic lamina. J. Neurosci. *22*, 7088–7096.

Das Sarma, J., Meyer, R. A., Wang, F., Abraham, V., Lo, C. W., and Koval, M. (2001). Multimeric connexin interactions prior to the trans-Golgi network. J. Cell Sci. *114*, 4013–4024.

Delmar, M., Stergiopoulos, K., Homma, N., Calero, G., Morley, G., Ek-Vitorin, J. F., and Taffet, S. M. (2000). A molecular model for the chemical regulation of connexin43 channels: the "ball-and-chain" hypothesis. In: Gap Junctions. Molecular Basis of Cell Communication in Health and Disease, ed. C. Peracchia, Academic Press, San Diego, CA, 223–248.

Diez, J. A., Ahmad, S., and Evans, W. H. (1999). Assembly of heteromeric connexons in guinea-pig liver en route to the Golgi apparatus, plasma membrane and gap junctions. Eur. J. Biochem. *262*, 142–148.

Falk, M. M., Buehler, L. K., Kumar, N. M., and Gilula, N. B. (1997). Cell-free synthesis and assembly of connexins into functional gap junction membrane channels. EMBO J. *16*, 2703–2716.

Falk, M. M. (2000). Cell-free synthesis for analyzing the membrane integration, oligomerization, and assembly characteristics of gap junction connexins. Methods *20*, 165–179.

Frenzel, E. M., and Johnson, R. G. (1996). Gap junction formation between cultured embryonic lens cells is inhibited by antibody to N-cadherin. Dev. Biol. *179*, 1–16.

Gilboa, L., Forbes, A., Tazuke, S. I., Fuller, M. T., and Lehmann, R. (2003). Germ line stem cell differentiation in *Drosophila* requires gap junctions and proceeds via an intermediate state. Development1 *30*, 6625–6634.

Goodenough, D. A., Goliger, J. A., and Paul, D. L. (1996). Connexins, connexons, and intercellular communication. Annu. Rev. Biochem. *65*, 475–502.

Hertig, C. M., Butz, S., Koch, S., Eppenberger-Eberhardt, M., Kemler, R., and Eppenberger, H. M. (1996). N-cadherin in adult rat cardiomyocytes in culture. II. Spatio-temporal appearance of proteins involved in cell-cell contact and communication. Formation of two distinct N-cadherin/catenin complexes. J. Cell Sci. *109*, 11–20.

Jacobs, K., Todman, M. G., Allen, M. J., Davies, J. A., and Bacon, J. P. (2000). Synaptogenesis in the giant-fibre system of *Drosophila*: interaction of the giant fibre and its major motorneuronal target. Development *127*, 5203–5212.

Kistler, J., Goldie, K., Donaldson, P., and Engel, A. (1994). Reconstitution of native-type noncrystalline lens fiber gap junctions from isolated hemichannels. J. Cell Biol. *126*, 1047–1058.

Krishnan, S. N., Frei, E., Swain, G. P., and Wyman, R. J. (1993). Passover: a gene required for synaptic connectivity in the giant fiber system of *Drosophila*. Cell *73*, 967–977.

Lagree, V., Brunschwig, K., Lopez, P., Gilula, N. B., Richard, G., and Falk, M. M. (2003). Specific amino-acid residues in the N-terminus and TM3 implicated in channel function and oligomerization compatibility of connexin43. J. Cell Sci. *116*, 3189–3201.

Laird, D. W. (1996). The life cycle of a connexin: gap junction formation, removal, and degradation. J. Bioenerg. Biomembr. *28*, 311–318.

Lee, Y. S., and Carthew, R. W. (2003). Making a better RNAi vector for *Drosophila*: use of intron spacers. Methods *30*, 322–329.

Luo, Y., and Radice, G. L. (2003). Cadherin-mediated adhesion is essential for myofibril continuity across the plasma membrane but not for assembly of the contractile apparatus. J. Cell Sci. *116*, 1471–1479.

Martin, P.E.M., and Evans, W. H. (2004). Incorporation of connexins into plasma membranes and gap junctions. Cardiovasc. Res. *62*, 378–387.

Meyer, R. A., Laird, D. W., Revel, J. P., and Johnson, R. G. (1992). Inhibition of gap junction and adherens junction assembly by connexin and A-CAM antibodies. J. Cell Biol. *119*, 179–189.

Musil, L. S., and Goodenough, D. A. (1993). Multisubunit assembly of an integral plasma membrane channel protein, gap junction connexin43, occurs after exit from the ER. Cell *74*, 1065–1077.

Panchin, Y., Kelmanson, I., Matz, M., Lukyanov, K., Usman, N., and Lukyanov, S. (2000). A ubiquitous family of putative gap junction molecules. Curr. Biol. *10*, R473–R474.

Panchin, Y. V. (2005). Evolution of gap junction proteins–the pannexin alternative. J. Exp. Biol. *208*, 1415–1419.

Phelan, P. (2005). Innexins: members of an evolutionarily conserved family of gap-junction proteins. Biochim. Biophys. Acta *1711*, 225–245.

Phelan, P., Nakagawa, M., Wilkin, M. B., Moffat, K. G., O'Kane, C. J., Davies, J. A., and Bacon, J. P. (1996). Mutations in shaking-B prevent electrical synapse formation in the *Drosophila* giant fiber system. J. Neurosci. *16*, 1101–1113.

Phelan, P., *et al*. (1998a). Innexins: a family of invertebrate gap-junction proteins. Trends Genet *14*, 348–349.

Phelan, P., and Starich, T. A. (2001). Innexins get into the gap. Bioessays *23*, 388–396.

Phelan, P., Stebbings, L. A., Baines, R. A., Bacon, J. P., Davies, J. A., and Ford, C. (1998b). *Drosophila* Shaking-B protein forms gap junctions in paired *Xenopus* oocytes. Nature *391*, 181–184.

Segretain, D., and Falk, M. M. (2004). Regulation of connexin biosynthesis, assembly, gap junction formation, and removal. Biochim. Biophys. Acta *1662*, 3–21.

Shimohigashi, M., and Meinertzhagen, I. A. (1998). The shaking B gene in *Drosophila* regulates the number of gap junctions between photoreceptor terminals in the lamina. J. Neurobiol. *35*, 105–117.

Söhl, G., and Willecke, K. (2004). Gap junctions and the connexin protein family. Cardiovasc. Res. *62*, 228–232.

Spradling, A. C., and Rubin, G. M. (1982). Transposition of cloned P elements into *Drosophila* germ line chromosomes. Science *218*, 341–347.

Stebbings, L. A., Todman, M. G., Phelan, P., Bacon, J. P., and Davies, J. A. (2000). Two *Drosophila* innexins are expressed in overlapping domains and cooperate to form gap-junction channels. Mol. Biol. Cell *11*, 2459–2470.

Stebbings, L. A., Todman, M. G., Phillips, R., Greer, C. E., Tam, J., Phelan, P., Jacobs, K., Bacon, J. P., and Davies, J. A. (2002). Gap junctions in *Drosophila*: developmental expression of the entire innexin gene family. Mech. Dev. *113*, 197–205.

Tazuke, S. I., Schulz, C., Gilboa, L., Fogarty, M., Mahowald, A. P., Guichet, A., Ephrussi, A., Wood, C. G., Lehmann, R., and Fuller, M. T. (2002). A germline-specific gap junction protein required for survival of differentiating early germ cells. Development *129*, 2529–2539.

Tepass, U., Gruszynski-DeFeo, E., Haag, T. A., Omatyar, L., Torok, T., and Hartenstein, V. (1996). Shotgun encodes *Drosophila* E-cadherin and is preferentially required during cell rearrangement in the neurectoderm and other morphogenetically active epithelia. Genes Dev. *10*, 672–685.

Tepass, U., Tanentzapf, G., Ward, R., and Fehon, R. (2001). Epithelial cell polarity and cell junctions in *Drosophila*. Annu. Rev. Genet *35*, 747–784.

Uemura, T., Oda, H., Kraut, R., Hayashi, S., Kotaoka, Y., and Takeichi, M. (1996). Zygotic *Drosophila* E-cadherin expression is required for processes of dynamic epithelial cell rearrangement in the *Drosophila* embryo. Genes Dev. *10*, 659–671.

Watanabe, T., and Kankel, D. R. (1992). The l(1)ogre gene of *Drosophila melanogaster* is expressed in postembryonic neuroblasts. Dev. Biol. *152*, 172–183.

Wei, C., Xu, X., and Lo, C. W. (2004). Connexins and cell signaling in development and disease. Annu. Rev. Cell Dev. Biol. *20*, 811–838.

Wei, C., Francis, R., Xu, X., and Lo, C. W. (2005). Connexin43 associated with an N-cadherin-containing multiprotein complex is required for gap junction formation in NIH3T3 cells. J. Biol. Chem. *280*, 19925–19936.

Wheelock, M. J., and Johnson, K. R. (2003). Cadherins as modulators of cellular phenotype. Annu. Rev. Cell Dev. Biol. *19*, 207–235.

White, T. W., Wang, H., Mui, R., Litteral, J., and Brink, P. R. (2004). Cloning and functional expression of invertebrate connexins from *Halocynthia pyreformis*. FEBS Lett. *577*, 42–48.

Xiao, H., Hrdlicka, L. A., and Nambu, J. R. (1996). Alternate functions of the single-minded and rhomboid genes in development of the *Drosophila* ventral neuroectoderm. Mech. Dev. *58*, 65–74.

Zhang, Z., Curtin, K. D., Sun, Y. A., and Wyman, R. J. (1999). Nested transcripts of gap junction gene have distinct expression patterns. J. Neurobiol. *40*, 288–301.

Zuppinger, C., Schaub, M. C., and Eppenberger, H. M. (2000). Dynamics of early contact formation in cultured adult rat cardiomyocytes studied by N-cadherin fused to green fluorescent protein. J. Mol. Cell Cardiol. *32*, 539–555.